SYMPOSIUM ON THE STABILITY AND OXIDATION CHEMISTRY
OF MIDDLE DISTILLATE FUELS
PRESENTED BEFORE THE DIVISIONS OF FUEL
AND PETROLEUM CHEMISTRY, INC.
AMERICAN CHEMICAL SOCIETY
WASHINGTON MEETING, AUGUST 26-31, 1990

A THREE-DIMENSIONAL ANALYSIS OF THE FLOW AND TEMPERATURE DISTRIBUTIONS IN THE JFTOT

By

J. A. Pearce and W. M. Roquemore
WRDC Aero Propulsion and Power Laboratory, Wright-Patterson AFB, Ohio, 45433

and

C. H. Oh, B. J. Merrill, and R. P. Wadkins
Idaho National Engineering Laboratory, P. O. Box 1625, Idaho Falls, Idaho 83415

ABSTRACT

This paper provides an insight into the detailed flow and temperature distributions in the Jet Fuel Thermal Oxidation Tester (JFTOT), a test device that has been used for many years to quantify the thermal stability of aircraft fuels. Though the JFTOT has found wide application as a qualification test device, very little is known about the many intricacies and nuances of the JFTOT flow field. Of particular interest is the possibility that variations in the flow field could be manifested in terms of changes in deposition on the JFTOT heater tube. To quantify the flow and temperature distributions, a three-dimensional numerical analysis is applied using the KIVA code. Also included in the analysis is a simplified model for jet fuel thermal degradation. Due to the limited amount of quantitative data available from JFTOT experiments, the deposition model used in the study is a global type Arrhenius equation with "calibration" data derived from tests with the Fiber Optic Modified JFTOT (FOM-JFTOT).

NOMENCLATURE

a_i constants in temperature curve fit
A_d Arrhenius preexponential factor
A_e exit flow area
A_i inlet flow area
D characteristic diameter

E_d Arrhenius activation energy
i grid representation of r
j grid representation of θ
k grid representation of z
K deposit thermal conductivity
l starting length
r radial direction
r_i inner radius
r_o outer radius
Δr $r_o - r_i$; channel width
Re_D Reynolds number based on hydraulic diameter
t time
T temperature
u_r radial velocity component
u_z axial velocity component
u_θ azimuthal velocity component
z axial direction
θ azimuthal direction
τ deposit thickness

INTRODUCTION

Thermal stability of jet fuels is a research area which has received significant attention for more than 30 years. Current interest in the field is high due to the prospects for future thermal stability challenges. These challenges arise primarily from the practice of using fuel to cool critical on-board aircraft systems. Large thermal stresses on the fuel are the consequence of this practice, and this condition is expected to worsen with increasingly sophisticated aircraft design. To further aggravate the problem, crude stock quality is expected to decrease in the future with possible deleterious effects on fuel thermal stability (1). At this juncture it has become critical to better understand the mechanisms that affect a fuel's thermal stability. The consequences of failing to gain a better understanding of thermal stability could include limiting aircraft performance envelopes for lack of suitably stable fuels.

A long standing tool of the thermal stability researcher is the Jet Fuel Thermal Oxidation Tester (JFTOT). This device has long been used by laboratories in the qualification of jet fuel thermal stability. Full details on the test procedures are not

necessary for the current discussion but can be found in the literature (2,3). A qualification test for a typical aviation fuel such as JP-4, JP-5, or JP-8 consists of flowing the given fuel around an electrically heated tube for a period of 150 minutes at a peak heater tube temperature of 260°C. The test is evaluated by comparing the color of the deposit on the heated tube to a standard reference. A numerical value or rating is assigned to the test results based on the tube coloration. Based on this rating a fuel either "passes" or "fails" the test. Unfortunately, the qualification test yields little or no data which can be used to better understand the various detailed mechanisms contributing to the degradation of fuel within the device.

In an attempt to try to increase the research value of JFTOT testing, variations on the standard qualification test have been devised (4). A common practice is to run tests at progressively higher tube temperatures until a "failure" is recorded. The temperature at which a fuel "fails" the test has been designated as the *Breakpoint Temperature*. Though this type of test certainly has more value than the qualification test, it still provides little information which could be valuable in the study of detailed degradation mechanisms.

Recent attempts have been made to try to quantify the results of JFTOT tests in terms which are more valuable to researchers (4-6). These tests have focused on examining the effects that various subprocesses have on the overall deposition process. Among the factors examined in these studies are fuel flow rate, tube temperature, and heater tube metallurgy. One of the more interesting results taken from the tests of Warner and Biddle (4) was a marked azimuthal asymmetry in the deposition on the tube. This trend was repeated in subsequent testing and is believed to be strongly linked to the complex flow field which exists within the JFTOT. Therefore, an exercise which may help to elucidate deposit mechanisms within the JFTOT is a determination of the detailed flow field within the device. The work presented here is focused on obtaining a description of the flow field within the JFTOT.

JFTOT GEOMETRY AND BOUNDARY CONDITIONS

JFTOT Geometry

A thorough understanding of the JFTOT geometry is necessary to comprehend the results which will be subsequently presented. The JFTOT is intended to be a simple flowing device for the qualification of jet fuels; however, a close examination of the flow passage reveals much about the JFTOT flow which is not simple. The Reynolds number at the tube entrance, based on the hydraulic diameter, is $Re_D \cong 13$. This Reynolds number places this flow firmly in the domain of laminar flow. The low Reynolds number is a

product of both the low flow rate through the JFTOT (3 ml/min) and the small annular flow channel (Δr < 1 mm). A schematic representation of the JFTOT is provided as Figure 1 to aid in demonstrating this point; also, the coordinate system (cylindrical) which is utilized for all subsequent discussions is provided as Figure 2.

The primary flow direction in the JFTOT is the axial (+z) direction; however, the flow is not a simple annular pipe flow as one might expect. Complexities arise in the JFTOT flow which are directly attributable to the orientation of the fuel inlet and exit. The fuel enters the JFTOT in the radial direction; consequently, the entry is normal to the primary flow direction (+z). This orientation of the flow, as it is introduced to the JFTOT, then provides a great deal of complication to the otherwise simple flow field. Also note that the entering flow impinges on a step in the JFTOT tube which further complicates the flow. Therefore, components of velocity in the r and θ directions in the lower region of the tube are introduced by the incoming fuel.

The flow is similarly perturbed by the fuel exit which is again situated normal to the primary flow direction. Since the JFTOT flow is elliptic in nature, the influence of a downstream disturbance will be manifested upstream of the exit; therefore, the effects of the exit orientation should be apparent in the region of the JFTOT upstream from the exit. Also, in a manner similar to the entering flow, the exiting flow must flow past a step on leaving the flow channel.

A further element complicating the JFTOT geometry is the respective orientation of the inlet and exit planes. The fuel is introduced in the -r direction at the location $\theta = 0°$, while the fuel exits in the +r direction at the location $\theta = 90°$. Therefore, there is a 90° rotation in the azimuthal plane from the inlet to the exit and an azimuthal (θ) component of velocity must be introduced to the flow to account for this rotation. In light of the previous discussions, it should now be apparent that the flow in the JFTOT is three-dimensional and quite complex, and the analysis of the flow field is not a trivial problem.

Boundary Conditions

One aspect critical to the determination of the JFTOT flow field is the application of proper boundary conditions. The primary quantities of interest are the velocity components and the fuel temperature. The following boundary conditions apply at the tube inlet:

$$r = r_o = 2.3125\text{x}10^{-3}\text{ m};\ \theta = 0°;\ z = 0$$
$$u_r = -0.01\text{ m/s};\ u_\theta = 0;\ u_z = 0$$
$$T = T_{amb} = 300\text{ K} \qquad 1)$$

Conditions at the tube exit ($r = r_o$, $\theta = 90°$, $z = 0.06$ m) are determined by the code and are unspecified at the outset. However, there is a constraint that the exiting velocity be in the $+r$ direction.

At the outer radius of the tube (excepting the inlet and exit), the following conditions apply:

$$r = r_o = 2.3125 \times 10^{-3} \text{ m}$$
$$u_r = u_\theta = u_z = 0$$
$$T = T_{amb} = 300 \text{ K} \qquad 2)$$

Admittedly, the temperature boundary condition at the outer radius is likely incorrect. In reality, the outer surface is exposed to ambient air, but it is certainly heated by both conduction through the test apparatus and convection from the heated fuel. However, since no reliable measurements of the outer housing temperature were available, the boundary was fixed at the ambient air temperature.

Finally, at the inner radius (JFTOT heater tube outer surface) the following conditions apply:

$$r = r_i = 1.40 \times 10^{-3} \text{ m}$$
$$u_r = u_\theta = u_z = 0$$
$$T \text{ (see (3))} \qquad 3)$$

Note that the ASTM (3) description of the JFTOT test provides axial temperature profiles along the heater tube. There is no azimuthal variation in these prescribed temperature profiles. For the particular case modeled in this study (maximum heater tube temperature of 550°F), a curve fit of the heater tube temperature profile was employed with the following form:

$$T(\text{K}) = a_1 + a_2 z + a_3 z^2 + a_4 z^3 \qquad 4)$$

where z is in mm and the constants a_i are

$$a_1 = 519.6 \text{ K}$$
$$a_2 = -3.676 \text{ K/mm}$$
$$a_3 = 0.2718 \text{ K/mm}^2$$
$$a_4 = -0.003857 \text{ K/mm}^3$$

NUMERICAL MODEL

Computational Fluid Dynamics

The fluid flow in the JFTOT was modeled using the KIVA code developed at the Los Alamos National Laboratory. The partial differential equations solved in the KIVA code are the Navier-Stokes, conservation of mass, and internal energy equations. The code is both three-dimensional and transient. For these calculations, JP-5 fuel was the fluid of interest; consequently, temperature dependent curve fits of the fluid properties were derived from existing data (7) and implemented into the code. Details of the numerical scheme employed in the code can be found in the literature (8-12), and their inclusion here is unnecessary.

The computational grid applied to the given problem is shown in Figures 3 and 4. Figure 3 shows a three-dimensional representation of the grid which consists of 8 radial cells, 24 azimuthal cells, and 24 axial cells (4,608 total cells). The coordinate orientations are supplied in the figure, as are the general locations of the fuel inlet and exit. Figure 4, which depicts an r-θ plane of the grid, further clarifies the geometry. Fuel is inlet in the azimuthal (j) cells between $j = 3$ and $j = 7$. The fuel exits between cells $j = 9$ and $j = 13$. Logically, the inlet is at the bottom of the computational grid at axial (k) cells $k = 1$ and $k = 2$, and the exit is at the top of the computational grid at $k = 24$ and $k = 25$. All fuel enters and exits the flow domain at the outer radius which corresponds to the radial (i) location $i = 9$. By specifying the inlet and exit regions in this manner, the correct flow areas of $A_i = A_e = 4.91 \times 10^{-6}$ m^2 are preserved in the model.

Jet Fuel Thermal Degradation

The calculation of jet fuel thermal degradation, in terms of a deposit thickness on the JFTOT heater tube, was accomplished separately from the KIVA code. A number of assumptions were made regarding the deposition on the heater tube; primarily that the deposition was solely a function of the temperature at the deposit/fuel interface and that the local flow field had *no* effect on the deposition. Due to a severe lack of quantitative deposition data from the JFTOT, a simple global Arrhenius expression was used to model the accumulation of deposits on the heater tube. The expression governing deposit growth is given by

$$\frac{d\tau}{dt} = A_d \, exp\left(\frac{-E_d}{T}\right) \qquad 5)$$

The preexponential factor (A_d) and activation energy (E_d) were determined from data provided by Warner and Biddle (4) with the Fiber Optic Modified JFTOT (FOM-JFTOT). From this data the following constants for the preexponential factor and activation energy were determined:

A_d = 155,970 m/s
E_d = 19,920 K

The temperature used in Equation 5 is the temperature at the fuel/deposit interface. This temperature is determined by analyzing the following energy equation for heat transfer in the deposit layer:

$$\left[\frac{1}{r}\frac{\partial}{\partial r}\left(Kr\frac{\partial T}{\partial r}\right)+\frac{1}{r^2}\frac{\partial}{\partial \theta}\left(K\frac{\partial T}{\partial \theta}\right)\right]=0 \qquad 6)$$

The boundary conditions for this equation, which is solved separately from KIVA, are taken from the KIVA temperature field for a given time step in the calculation.

RESULTS

JFTOT Flow Field

Though the KIVA code calculates the flow field in a transient sense, all of the velocity vectors and temperature contours displayed are for an instant in time subsequent to the system achieving a steady state. The first depiction of the flow field is provided as Figure 5. On the left are contours of the fluid temperature and on the right are velocity vectors. The three slices of the flow field shown are r-θ planes at the bottom (z = 0), mid-height (z = 0.03 m), and top (z = 0.06 m) of the flow domain. Note the orientation of the inlet and exit with respect to the plots which are shown (refer to Figures 3 and 4).

First considering the plots of the isotherms, note that for each plot the minimum and maximum temperatures are given below the figure and the contours are evenly spaced throughout the given temperature range. At the bottom of the domain note how the contour lines are bunched near the surface of the tube on the side corresponding to the fluid inlet. This bunching indicates steep thermal gradients and is a consequence of the entering fluid. On the side of the tube opposite from the inlet, note how the contour lines are much more widely spaced indicating the penetration of thermal energy into the flow. This is a consequence of the nearly stagnant flow in this region of the domain.

The temperature contours at the mid-height appear to be evenly distributed both radially and azimuthally. This is apparently because the thermal energy has sufficiently penetrated the fuel to eliminate any significant radial or azimuthal variations in the temperature field which were caused by the inlet. Furthermore, at this plane the flow is farthest from any of the influences which tend to perturb the flow (i. e., the inlet and exit). Moving to the exit, the contours are evenly spaced excepting the region where the fuel is exiting. At the exit, the contours appear to be stretched by the influence of the exiting flow.

Before discussing the velocity vectors depicted in Figure 5, some explanatory notes are necessary. First, since these depictions are r-θ planes, no axial velocity component is visible in these plots. Second, the plot routine scales the vectors independently for each plot; therefore, the length of the vectors is an indicator of velocity magnitude only for a given plot. The magnitudes of vectors *are not* directly related from plot to plot.

In the plot at the bottom of the domain, the influence of the incoming fluid can clearly be seen. There is an expected high radial component of velocity near the inlet, and there is also a high azimuthal velocity away from the inlet. However, on the side of the tube opposite the inlet the radial and azimuthal velocity components are very small. Moving to the mid-height, the flow is considerably more complex. Even at the mid-height, the influence of the exit can already be seen in terms of an outward radial component of velocity. However, note that the magnitude of these vectors is approaching the limits of the code's numerical accuracy. Directly opposite the azimuthal location of the exit, the azimuthal velocity component is again very small. Away from this location in both directions is a large azimuthal component of velocity. In some regions, there is also evidence of recirculation.

Finally, moving to the tube exit, the flow appears to be much more well ordered. There is a strong outward radial component of velocity at the exit, and there is also a significant azimuthal component of velocity on the side of the tube corresponding to the exit. However, on the opposite side of the tube, both the radial and azimuthal velocity components appear to be minute.

Moving to another view of the flow field, Figure 6 depicts radial profiles of temperature and axial velocity at the same axial locations used in Figure 5. Note that each of the plots in Figure 6 is at the azimuthal location corresponding to the fuel exit ($\theta = 90°$). In the three temperature plots, the penetration of thermal energy can be seen progressively as one moves up the tube. At the bottom of the tube, there is a large radial gradient in temperature near the heater tube surface, and this effect is diminishing at the mid-height. At the tube exit, the slope is in fact very shallow, indicating a low rate of heat transfer to the fluid.

The velocity plots show basically an expected result. Note that the influences of radial and azimuthal velocity components are not present in this figure. At both the bottom of the tube and the mid-height, the velocity profiles are basically parabolic. This is the type of behavior that would be expected in a developed laminar pipe flow. Note that for laminar pipe flows, the length required for a flow to develop is approximately

$$l = 0.058\, Re_D\, D \qquad 7)$$

which for $Re_D \cong 13$ equates to approximately $0.75D$ (13). Assuming D is the hydraulic diameter, the entire length of the JFTOT is approximately $160D$. This implies that the flow becomes developed a short distance from the inlet. Admittedly, the geometry of the JFTOT is not the specific geometry to which this relationship applies; however, even if this relationship were in error by two orders of magnitude, the flow would still be developed at the tube mid-height. Finally, the profile at the top of the domain appears to have an anomaly at the outer radius where the velocity is not zero. This is simply due to the presence of the fuel exit.

The final figure of the flow field is given as Figure 7. This plot depicts the velocity vectors in an r-z plane of the flow domain. The plot on the left represents the azimuthal positions corresponding to the exit ($\theta = 90°$ and 270°) and the plot on the right represents the positions corresponding to the inlet ($\theta = 0°$ and 180°). At the inlet ($\theta = 0°$), the influence of the entering fluid can clearly be seen, as can the flow stagnation in all other regions. Through the middle section of the tube there is little to note. Due to the great magnitude of the axial velocity with respect to the radial velocity ($u_z/u_r >> 1$) in most regions of the flow field, the influence of the radial velocity is not apparent. Finally, at the exit ($\theta = 90°$) the influence of the exiting flow is evident, and the flow is basically stagnant in all other regions.

Jet Fuel Thermal Degradation

The results of the calculation of deposit thickness on the JFTOT heater tube are given in Figure 8. Axial profiles of both the deposit thickness and wall temperature are shown. The results clearly show that the growth of the deposit layer follows the increase in wall temperature along the tube length. One would certainly expect this when considering that the model for deposit growth is based solely on the temperature of the fuel/deposit interface (Equation 5). The maximum deposit occurs at the location of the maximum temperature, and the maximum deposit thickness of 0.13 μm compares favorably with the measured value of 0.14 μm (4). It appears that this deposition model does a reasonable job of

approximating the JFTOT deposition for the specific case for which it was devised. However, its applicability to any other thermal stability experiments is questionable, and further studies would have to be accomplished to make any determination.

The premise that the local fluid flow has no influence on the deposition process is most certainly incorrect. Though many experiments have substantiated the significant role that surface temperature plays in the deposition process, it is not the sole contributing factor in jet fuel degradation. Some models have recently been presented that have addressed the issue of including multiple reaction steps in the degradation chemistry and allowing for the influence of fluid flow and bulk fuel temperature on the overall deposition process (14-16). However, the complexity of these models was beyond the scope of the current modeling effort, which was primarily focused on a determination of the JFTOT flow field.

CONCLUSIONS AND RECOMMENDATIONS

The results presented here have clearly demonstrated that the flow field in the JFTOT is quite complex. Due to the orientation of the flow inlet and exit, elements of flow in the radial and azimuthal directions are evident throughout the entire flow field. If one assumes that the flow field has some bearing on the deposition process, this complication of the flow could have a significant effect on the deposition observed on the JFTOT heater tube. However, the effects that the radial and azimuthal flow disturbances have on the deposition are not clear.

Further experimental efforts are necessary to elucidate the various mechanisms of fuel thermal degradation. Both the complex degradation chemistry and the effects of fluid mechanics and heat transfer must be addressed to better understand the overall deposition process. The most difficult task appears to be designing experiments that can isolate particular chemical and transport processes. Clearly the JFTOT is not such a device. Even though the JFTOT has been of great value in the qualification of fuel thermal stability, its use as a research tool is of questionable value.

ACKNOWLEDGEMENTS

This effort was jointly supported by the WRDC Aero Propulsion and Power Laboratory and the Department of Energy (DOE) Pittsburgh Energy Technology Center. The authors wish to thank Dr. Nand K. Narain, the DOE-Pittsburgh Program Manager, and William E. Harrison III, the U. S. Air Force Program Manager, for their guidance in this effort.

LITERATURE CITED

(1) TeVelde, J. A. , and Glickstein, M. R. , United Technologies/Pratt & Whitney, NAPC-PE-87C (1983).

(2) Alcor, Inc., Report No. 75-167 (1975).

(3) ASTM D 3241-82, *1985 Annual Book of ASTM Standards: Petroleum Products, Lubricants, and Fossil Fuels,* Volume 05.03, 150-172 (1985).

(4) Warner, P. A. and Biddle, T. B., United Technologies/Pratt & Whitney, Report No. FR 19032-11 (1988).

(5) Clark, R. H. and Thomas, L., "An Investigation of the Physical and Chemical Factors Affecting the Performance of Fuels in the JFTOT," SAE Aerospace Technology Conference and Exposition (1988).

(6) Kendall, D. R. and Mills, J. S., SAE Paper 851871 (1985).

(7) Nixon, A. C., Ackerman, G. H., Faith, L. E., Henderson, H. T., Ritchie, A. W., Ryland, L. B. , and Shryne, T. M., Shell Development Company, AFAPL-TR-67-114, Pt. III, Vol. II (1970).

(8) Amsden, A. A., Ramshaw, J. D., O'Rourke, P. J., and Dukowicz, J. K., Los Alamos National Laboratory, LA-10245-MS (1985).

(9) Amsden, A. A., Ramshaw, J. D., Cloutman, L. D., and O'Rourke, P. J., Los Alamos National Laboratory, LA-10534-MS (1985).

(10) O'Rourke, P. J. and Amsden, A. A., Los Alamos National Laboratory, LA-10849-MS (1986).

(11) Amsden, A. A., O'Rourke, P. J., and Butler, T. D., Los Alamos National Laboratory, LA-11560-MS (1989).

(12) Oh, C. H., Merrill, B. J., and Wadkins, R. P., Idaho National Engineering Laboratory, WRDC-TR-89-2138 (1989).

(13) Shames, Irving H., *Mechanics of Fluids*, New York, McGraw-Hill Book Company, 270 (1982).

(14) Roquemore, W. M., Pearce, J. A., Harrison, W. E., III, Krazinski, J. L. , and Vanka, S. P., *Preprints - Division of Petroleum Chemistry 34* (4), 841-849 (1989).

(15) Deshpande, G. V., Serio, M. A., Solomon, P. R., and Malhotra, R., "Modeling of the Thermal Stability of Aviation Fuels," Symposium on the Chemical Aspects of Hypersonic Propulsion, 198th National Meeting of the ACS, Miami, FL (1989).

(16) Krazinski, J. L., Vanka, S. P., Pearce, J. A. , and Roquemore, W. M., ASME Paper No. 90-GT-33 (1990).

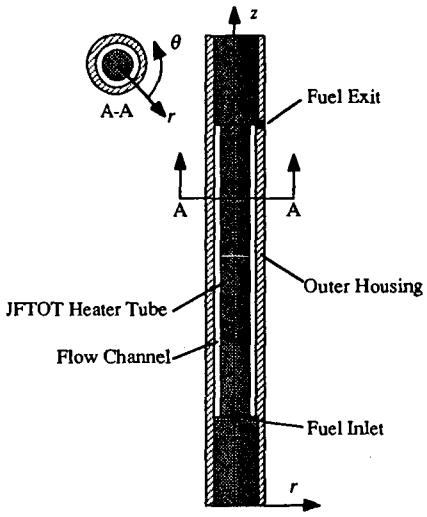

Figure 1: Schematic Representation of the JFTOT (Not to Scale)

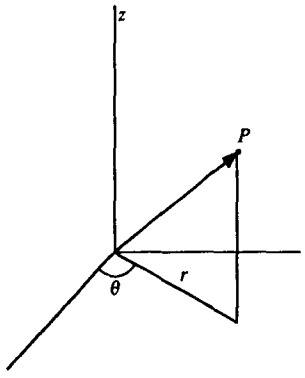

Figure 2: Cylindrical Coordinate System Used in KIVA Calculations

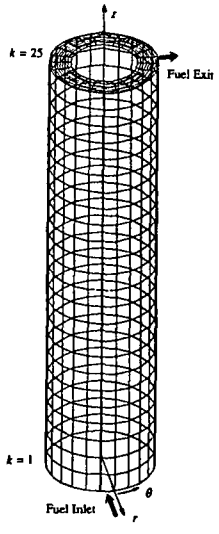

Figure 3: Three-Dimensional View of 8 x 24 x 24 Computational Grid

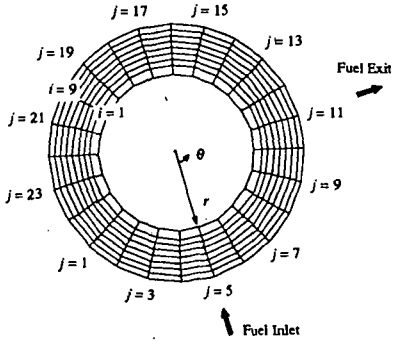

Figure 4: Top View of Computational Grid

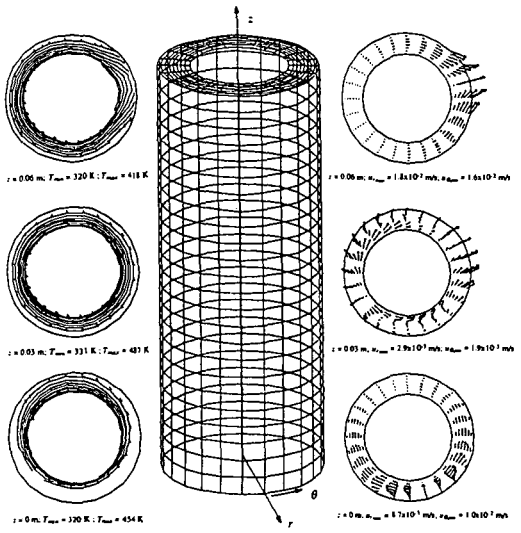

Figure 5: Calculated Temperature Contours and Velocity Vectors at the Bottom, Mid-Height, and Top of the JFTOT

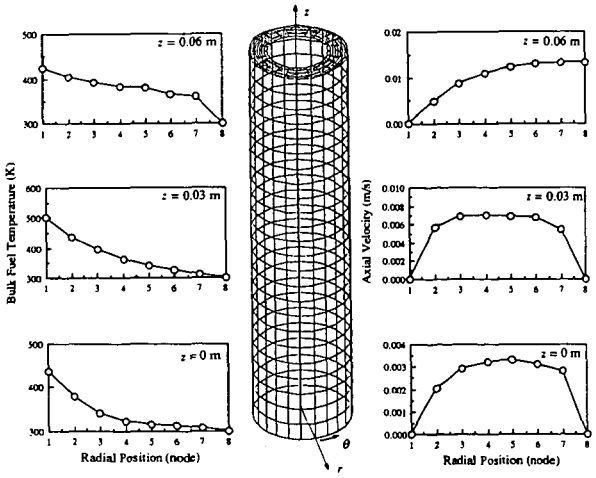

Figure 6: Calculate Radial Temperature and Axial Velocity Profiles at the Bottom, Mid-Height, and Top of the JFTOT

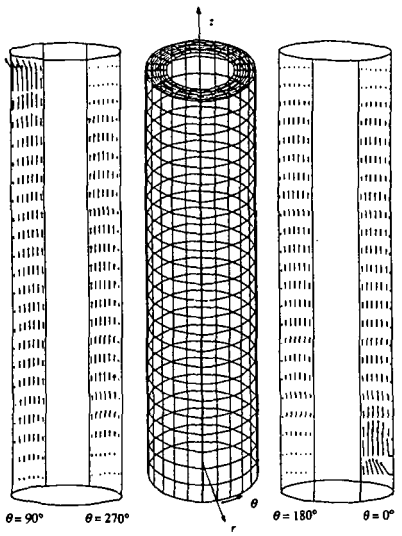

Figure 7: Calculated Velocity Vectors in the r-z Plane for Azimuthal Positions Corresponding to the Fuel Inlet and Exit

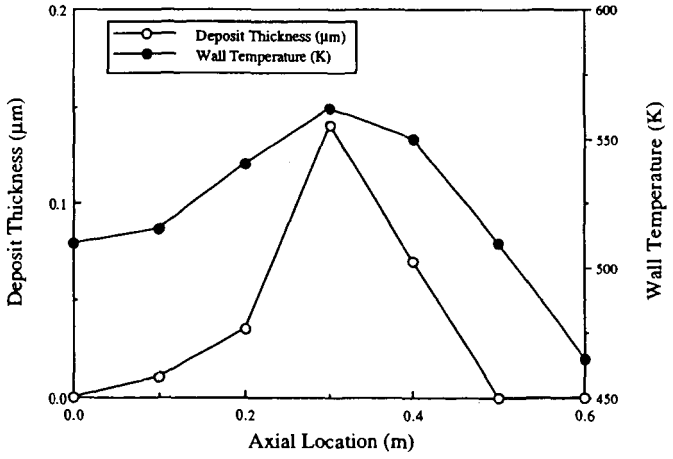

Figure 8: Predicted Axial Profiles of Deposit Thickness and Wall Temperature in the JFTOT